EARTHQUAKE ENGINEERING AND STRUCTURAL DYNAMICS
Earthquake Engng. Struct. Dyn. **28**, 609–631 (1999)

EXPERIMENTAL INVESTIGATION OF ADJACENT BUILDINGS CONNECTED BY FLUID DAMPER

Y. L. XU*, S. ZHAN, J. M. KO AND W. S. ZHANG
Department of Civil and Structural Engineering, The Hong Kong Polytechnic University, Hung Hom, Kowloon, Hong Kong

SUMMARY

Dynamic characteristic and harmonic response of adjacent buildings connected by fluid damper were experimentally investigated using model buildings and fluid damper. Two building models were constructed as two three-storey shear buildings of different natural frequencies. Model fluid damper connecting the two buildings was designed as linear viscous damper of which damping coefficient could be adjusted. The two buildings without fluid dampers connected were first tested to obtain their individual dynamic characteristics and responses to harmonic excitation. The tests were then carried out to determine modal damping ratios of the adjacent buildings connected by the fluid damper of different damping coefficients and at different locations. Optimal damper damping coefficient and location for achieving the maximum modal damping ratio were thus found. The measured modal damping ratios and harmonic responses of the building-fluid damper system were finally compared with those from the individual buildings. The comparison showed that the fluid damper of proper parameter could significantly increase the modal damping ratio and tremendously reduce the dynamic response of both buildings. Copyright © 1999 John Wiley & Sons, Ltd.

KEY WORDS: experimental investigation; adjacent buildings; fluid damper; dynamic characteristic; harmonic response

INTRODUCTION

Buildings in a modern city are often built closely to each other because of limited land available. These buildings, in most cases, are separated without any structural connections or are connected rigidly at the ground level only. Hence, wind-resistant or earthquake-resistant capacity of each building mainly depends on itself. The concept of linking adjacent buildings together for response control using either passive dampers or active dampers has been thus presented.

Seto and Matsumoto[1] suggested using active actuators to connect a group of buildings to mitigate building motion and investigated how to prevent spillover problems. Yamada *et al.*[2] let

* Correspondence to: Y. L. Xu, Department of Civil and Structural Engineering, The Hong Kong Polytechnic University, Hung Hom, Kowloon, Hong Kong. E-mail: ceylxu@polyu.edu.hk

Contract/grant sponsor: Hong Kong Polytechnic University

CCC 0098–8847/99/060609–23$17·50

Received 16 September 1998

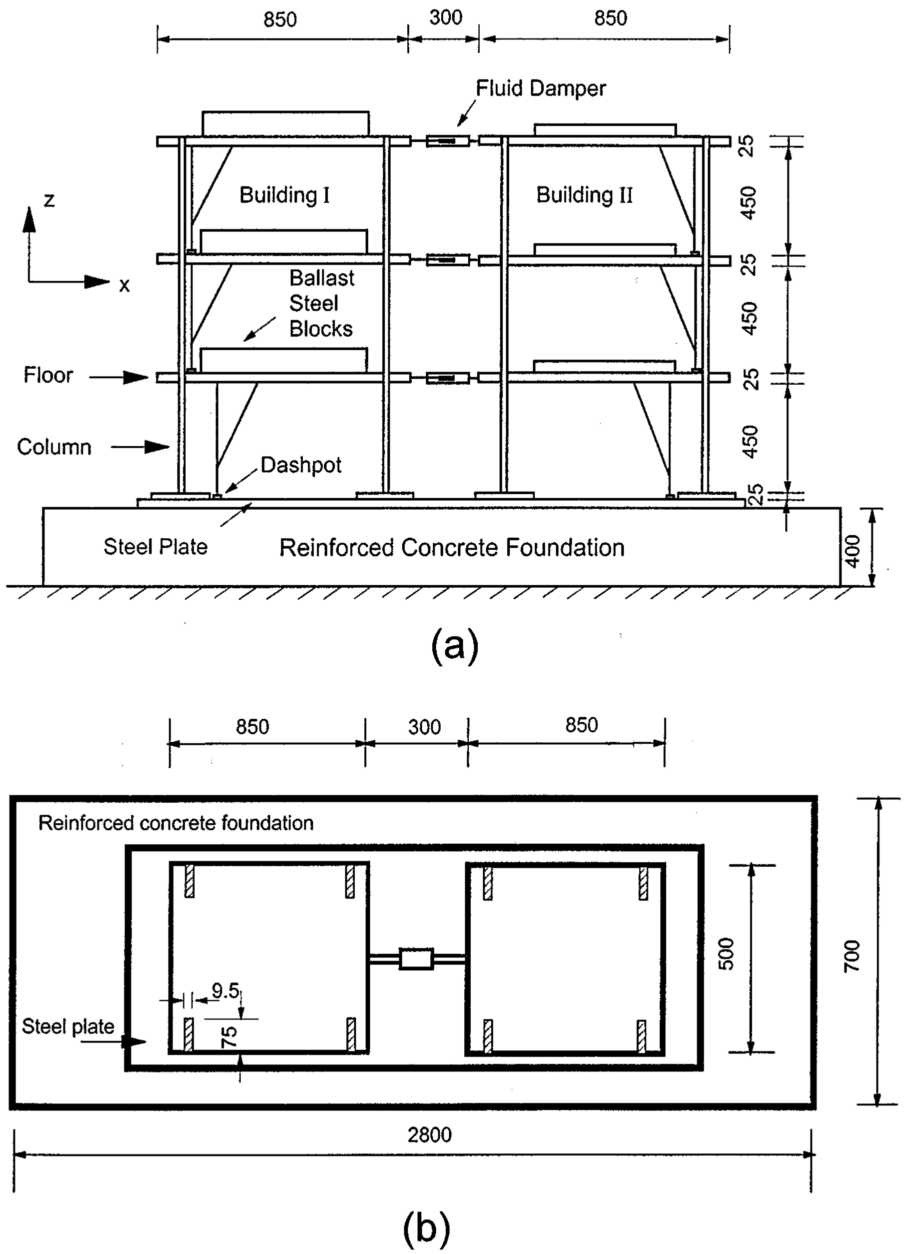

Figure 1. Configuration of adjacent building-fluid damper system: (a) elevations; (b) plan (all dimensions in mm)

active actuators generate negative stiffness so as to shift the natural frequencies of adjacent buildings away from the dominant frequency of ground motion. Apart from using active control technology, Gurley *et al.*[3] theoretically investigated the possibility of using a passively damped elastic link to couple adjacent buildings for control of response to wind. Xu *et al.*[4] theoretically

investigated the performance of adjacent buildings connected by a number of damped elastic links against earthquake. However, the problem has not been studied exhaustively with respect to the interaction of the controllers with the inherent properties of the building and the overall performance of the controller-building system. In particular, to the best of the writers' knowledge the experimental investigations on passive damper-connected adjacent buildings are very limited.

This paper thus presents an experimental study of adjacent buildings connected by fluid dampers using two three-storey building models and a linear viscous damper. The experimental arrangement, including the design of building models and the design and calibration of fluid damper model, is introduced first. The dynamic characteristics of individual buildings, obtained using system identification technique are then presented. Followed are the investigation of variations of modal damping ratio and natural frequency of the damper-building system to damper damping coefficient. Finally, the measured dynamic responses of the damper-building system to harmonic excitation are compared with those of individual buildings to evaluate the effectiveness of fluid damper and the overall performance of the damper-building system.

EXPERIMENTAL ARRANGEMENT

Building models

Two building models were designed and constructed as three-storey shear buildings in order to facilitate the system identification and the comparison with theoretical analysis at a late stage (see Figure 1). The steel frame of each building consisted of three rigid plates and four flexible columns. The plates and columns were welded properly to form rigid joints. The overall dimensions of each building were measured at 1450 mm $\times$ 850 mm $\times$ 500 mm. The two buildings were then welded in a tandem arrangement to a large reinforced concrete foundation that was in turn bolted into the massive concrete laboratory ground floor. The distance between the two buildings was set at 300 mm for the installation of fluid damper. The columns were made of high strength steel of 435 MPa yield stress and 200 GPa modulus of elasticity. The 9·5 mm $\times$ 75 mm cross-section of the column was arranged in such a way that the first natural frequency of each building was much lower in the x-direction than in the y-direction. This arrangement restricted the building motion in the x-direction and thus the building models were effectively reduced to planar frames in the x–z plane. The thickness of each steel floor (plate) was 25 mm so that the floor can be regarded as a rigid plate in horizontal, leading to a shearing type of deformation. By placing the additional mass on each floor of each building, the natural frequencies of each building can be changed. To properly simulate the inherent energy dissipation capacity of the real building, the small dashpots were installed between every two floors and the structural damping ratios of each building could be thus adjusted within a wide range.

Fluid damper

One objective of this experiment is to investigate variations of modal damping ratio and natural frequency of the damper-building system with damper damping coefficient. Thus, a viscous fluid damper that can be adjusted to have varying damping coefficient within a certain range is required. Such a fluid damper is hardly found in the market and therefore a plate fluid damper was designed and manufactured in the Hong Kong Polytechnic University. The plate fluid

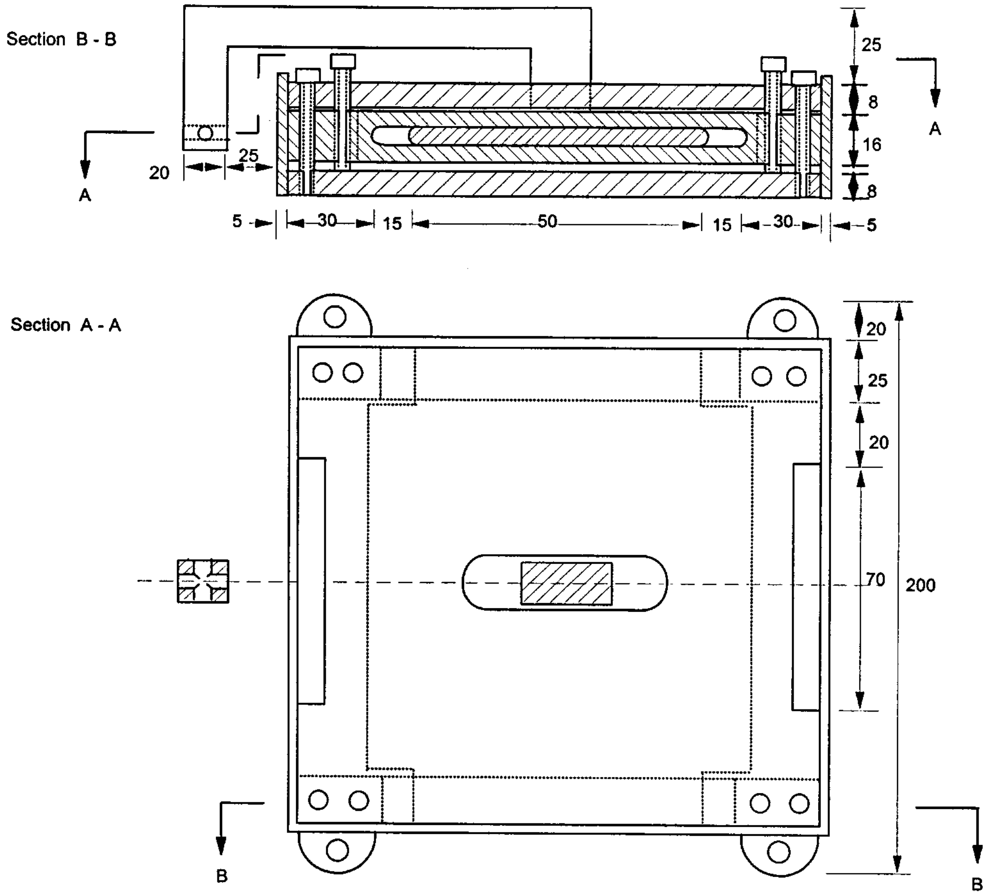

Figure 2. Configuragtion of plate fluid damper model

damper mainly consisted of a plate as a piston moving in a rectangular container filled with silicone coil (see Figure 2). The relative motion of the piston to the rectangular container sheared the fluid in the two gaps and provided energy dissipation. By adjusting the gaps between the plate and the top and bottom of the rectangular container and by changing oil viscosities as well, different damper damping coefficients were achieved. To obtain a linear viscous property, some openings were made in the top of the container to release the oil pressure caused by the motion of the piston.

The mechanical characteristics of the plate fluid damper were examined using the testing arrangement shown in Figure 3. An electrodynamic exciter (Link Dynamic System 409) was used under displacement control and it applied a sinusoidal motion to the piston of the plate fluid damper. The force in the damper was measured by a load cell that was connected to a reaction frame. The displacement of the damper piston was measured by a displacement transducer. Based on the measured load and displacement time histories, the mechanical characteristics of the damper could be determined. For steady-state conditions, the damper piston motion measured

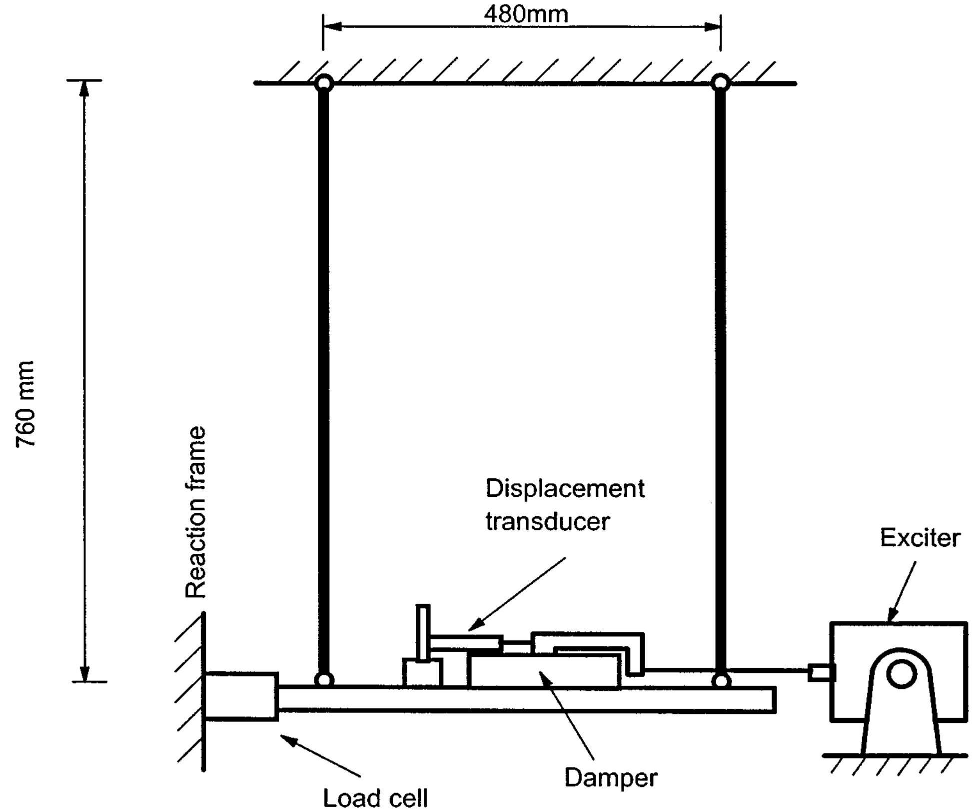

Figure 3. A calibration set-up for plate fluid damper model

from the displacement transducer and the damper force measured from the load cell can be, respectively, represented by

$$u = u_0 \sin(\omega t) \tag{1}$$

$$P = P_0 \sin(\omega t + \phi) = K_{d1} u_0 \sin(\omega t) + K_{d2} u_0 \cos(\omega t) \tag{2}$$

where u_0 is the amplitude of the piston displacement, ω is the frequency of motion, t is the time, P_0 is the amplitude of the damper force, ϕ is the phase angle and K_{d1} and K_{d2} are the storage stiffness and the loss stiffness, respectively. The loss stiffness can be determined from the measured damper force and displacement time histories using the following equation:

$$K_{d2} = \frac{P_0}{u_0} \sin\phi = \frac{\oint P\,\mathrm{d}u}{\pi u_0^2} \tag{3}$$

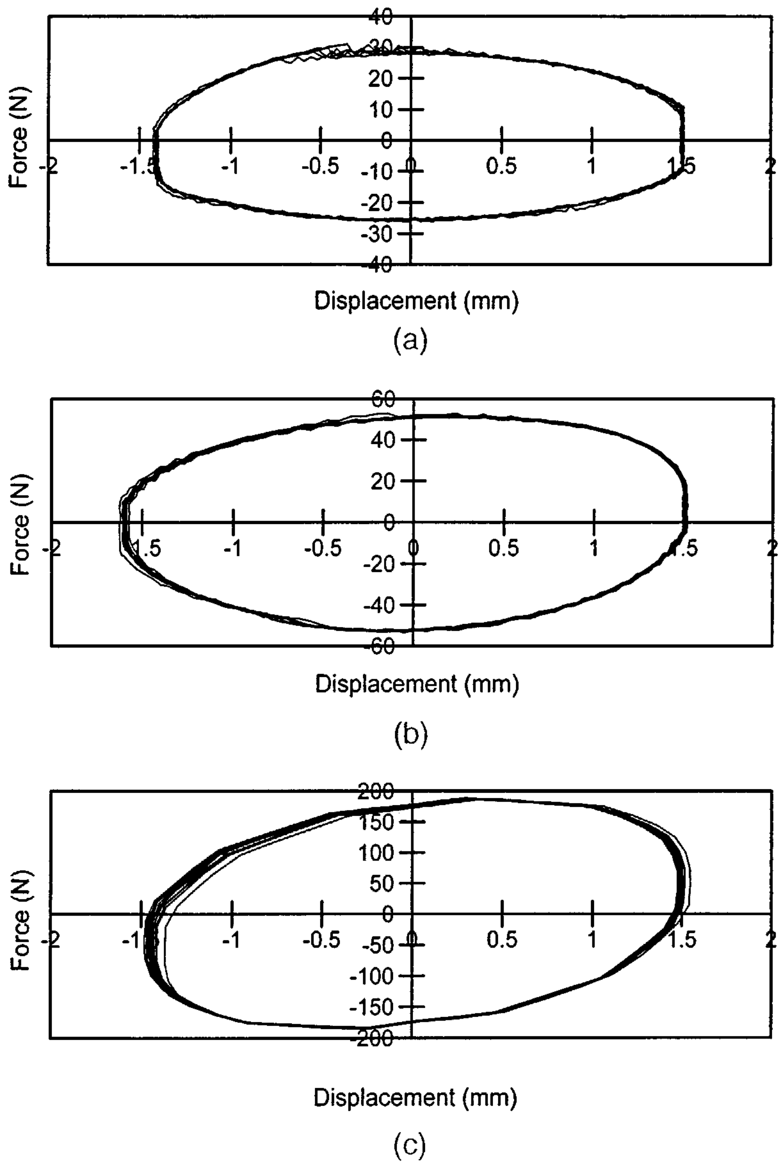

Figure 4. Recorded force–displacement loops of fluid damper. Motion frequency: (a) 1 Hz; (b) 2 Hz; (c) 10 Hz

The damper damping coefficient, the phase angle, and the storage stiffness can be then estimated by

$$C_{\mathrm{d}} = \frac{K_{\mathrm{d}2}}{\omega} \tag{4}$$

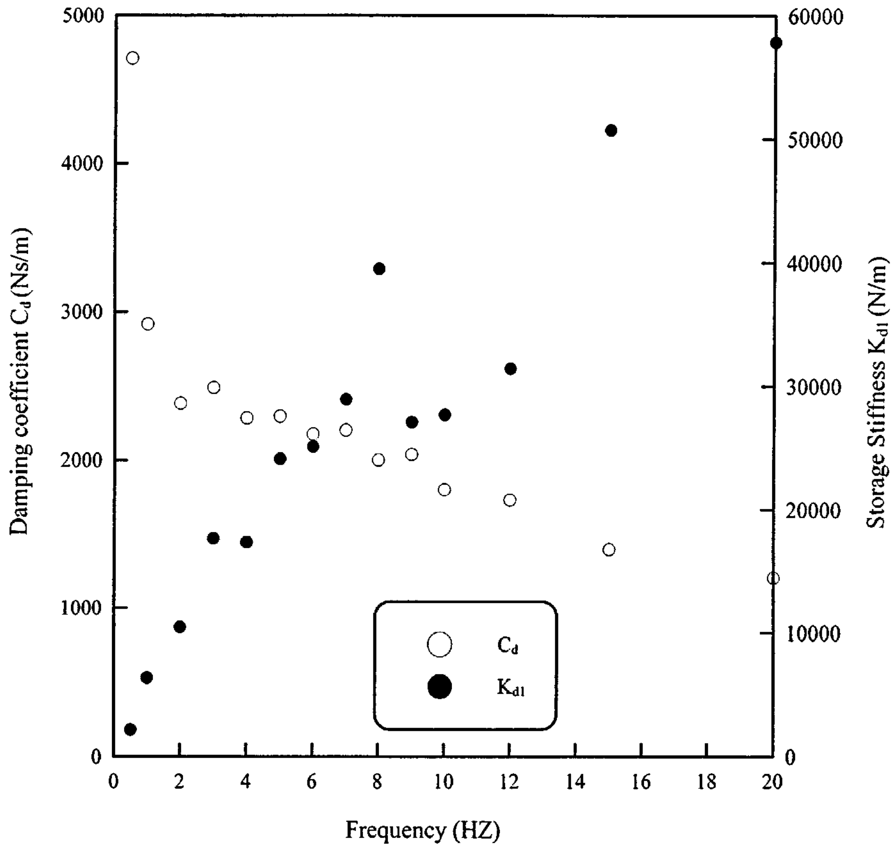

Figure 5. Variation of damping coefficient and storage stiffness with motion frequency

$$\phi = \sin^{-1}\left(\frac{K_{d2}u_0}{P_0}\right) \tag{5}$$

$$K_{d1} = \frac{P_0}{u_0}\cos\phi \tag{6}$$

Typical recorded force–displacement loops are presented in Figure 4 at a temperature of 25°C and frequencies of 1, 2 and 10 Hz, respectively. It was found that the plate fluid damper possesses small storage stiffness and large damping coefficient when the frequency is below 2 Hz and its behaviour is essentially linear viscous. When the frequency of damper motion is above 2 Hz, the damper exhibits a certain amount of storage stiffness and its behaviour is essentially viscoelastic. Figure 5 shows variations of damper damping coefficient and storage stiffness with the frequency of motion for the piston of displacement amplitude. With a frequency range of 2 to 7 Hz, damper damping coefficient remained almost constant, but as the motion frequency was further increased,

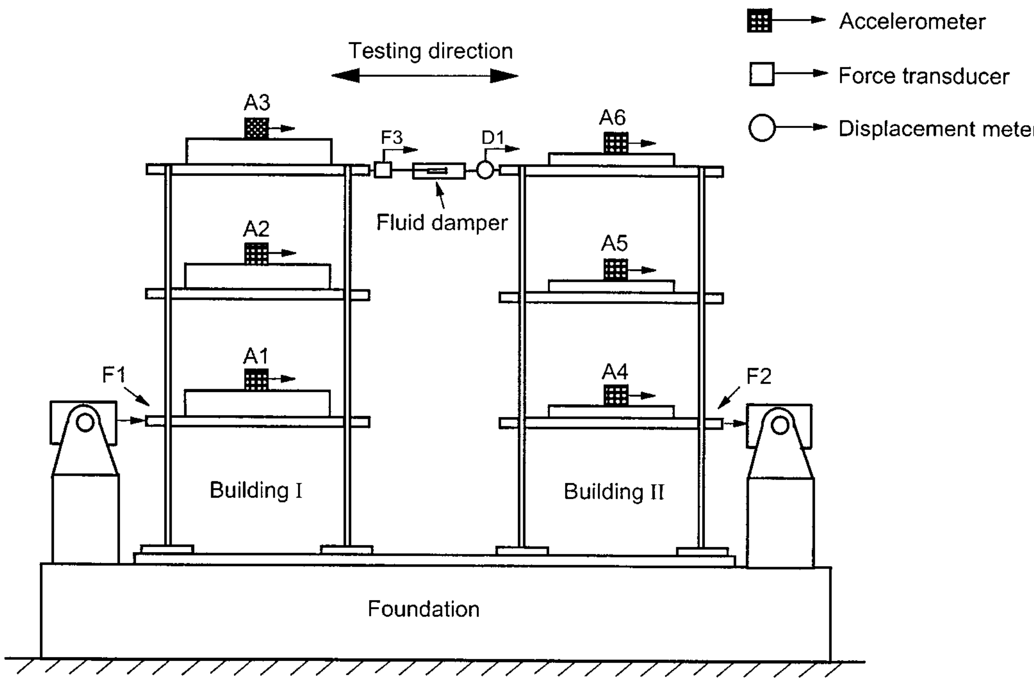

Figure 6. Instrumentation diagram

the damping coefficient started to decrease. The storage stiffness, on the other hand, increased with increasing frequency of motion. In addition, the mechanical properties of the plate fluid damper were much less affected by the amplitude of motion than the frequency of motion. This was confirmed in the tests conducted at the same frequency but in different amplitudes.

From the calibration of the plate fluid damper, it can be concluded that the plate fluid damper used in the tests has linear viscous behaviour when the motion frequency is less than 2 Hz and has viscoelastic behaviour when the motion frequency is above 2 Hz. These mechanical properties of the plate fluid damper are similar to the commercial fluid dampers manufactured by Tayler Devices, Inc. U.S.A. and calibrated by Constantinou and Symans.[5,6] The Maxwell model describing the commercial fluid dampers can be thus used for the plate fluid damper. This will be discussed elsewhere together with theoretical studies of the fluid damper-adjacent building system at a late stage.

Measurement and instrumentation

The natural frequencies of the reinforced concrete foundation were first measured using an instrumented hammer and several accelerometers after the foundation was built. The lowest natural frequency of the foundation in the x-direction (see Figure 1) was measured at 450 Hz, which was much higher than the concerned natural frequencies of two building models in the same direction. The high-frequency guaranteed that the foundation did not affect vibration tests of the buildings.

The measurement was then taken on each building to determine their natural frequencies, structural modal damping ratios, mode shapes, and responses to harmonic loading. This was achieved by installing one accelerometer on each floor in the x-direction and using the electrodynamic exciter to give the building a constant amplitude harmonic force within a wide range of excitation frequency (see Figure 6). The natural frequencies and structural modal damping ratios were identified from the recorded frequency response curves whilst the mode shapes were identified from the recorded response time histories of each floor at the resonance frequencies.

The plate fluid damper was then installed in the top floor, the second floor, and the first floor, respectively, to connect two buildings together. The dynamic responses of both buildings at each floor to harmonic excitation were measured simultaneously. The damper displacement, i.e. the relative displacement between the two buildings, and the damper force were also simultaneously measured using the load cell and displacement meter (see Figure 6), from which the damper damping coefficient could be directly estimated for different damper configurations used in the tests. To capture overall characteristics of the building-damper system, the external excitation harmonic force was applied to the first floor of Building I first and then to the first floor of Building II.

For each load case and each damper location, the optimal damper damping coefficient for achieving the maximum modal damping ratio of the system was sought. The building responses were recorded for the comparison with those of the buildings without damper connected.

STRUCTURAL PROPERTIES OF INDIVIDUAL BUILDINGS

The identification of the structural properties of two individual buildings without fluid damper connected was easily accomplished by the procedure described in the last section. For Building I, the mass of each floor was equal to 314·5 kg while the mass of each floor of Building II was 139·8 kg.

The measured first three natural frequencies were 2·92, 8·39 and 12·38 Hz for Building I and 4·50, 12·97 and 19·17 Hz for Building II. Clearly, the third natural frequency of Building I was very close to the second natural frequency of Building II. The first three modal damping ratios were estimated as 0·021, 0·026 and 0·027 for Building I and 0·019, 0·026 and 0·032 for Building II. The measured mode shape matrixes for Buildings I and II are listed as follows:

$$[\Psi]_1 = \begin{bmatrix} 1{\cdot}000 & 1{\cdot}000 & 1{\cdot}000 \\ 1{\cdot}771 & 0{\cdot}416 & -1{\cdot}170 \\ 2{\cdot}256 & -0{\cdot}787 & 0{\cdot}549 \end{bmatrix}, \quad [\Psi]_2 = \begin{bmatrix} 1{\cdot}000 & 1{\cdot}000 & 1{\cdot}000 \\ 1{\cdot}817 & 0{\cdot}437 & -1{\cdot}294 \\ 2{\cdot}258 & -0{\cdot}819 & 0{\cdot}616 \end{bmatrix} \tag{7}$$

The stiffness and damping matrixes of each building can be identified using the following equations:

$$[K] = [M]\left(\sum_{i=1}^{3} \frac{\omega_i^2}{m_i^*}\{\varphi_i\}\{\varphi_i\}^{\mathrm{T}}\right)[M] \tag{8}$$

$$[C] = [M]\left(\sum_{i=1}^{3} \frac{2\xi_i\omega_i}{m_i^*}\{\varphi_i\}\{\varphi_i\}^{\mathrm{T}}\right)[M] \tag{9}$$

The stiffness and damping matrixes identified for Buildings I and II are listed as follows:

$$[K]_1 = \begin{bmatrix} 12{\cdot}19 & -6{\cdot}14 & 0{\cdot}34 \\ -6{\cdot}14 & 11{\cdot}03 & -5{\cdot}75 \\ 0{\cdot}34 & -5{\cdot}75 & 5{\cdot}79 \end{bmatrix} \times 10^5 \text{ N/m} \tag{10}$$

$$[K]_2 = \begin{bmatrix} 11{\cdot}23 & -5{\cdot}92 & 0{\cdot}26 \\ -5{\cdot}92 & 11{\cdot}91 & -6{\cdot}30 \\ 0{\cdot}26 & -6{\cdot}30 & 6{\cdot}18 \end{bmatrix} \times 10^5 \text{ N/m} \tag{11}$$

$$[C]_1 = \begin{bmatrix} 1002 & -341 & -43 \\ -341 & 847 & -374 \\ -43 & -374 & 577 \end{bmatrix} \text{N s/m} \tag{12}$$

$$[C]_2 = \begin{bmatrix} 652 & -275 & -7 \\ -275 & 688 & -314 \\ -7 & -314 & 406 \end{bmatrix} \text{N s/m} \tag{13}$$

The identified matrixes indicate that the building models used in the tests can be regarded as shear-type buildings. These identified matrixes together with the identified parameters for fluid damper can be used to construct an analytical model for the studied fluid damper-adjacent building system.

CHARACTERISTIC OF DAMPER-BUILDING SYSTEM

Fluid damper at top floor

A fluid damper of damping coefficient of 3531 N s/m at a frequency of 3·24 Hz was used to connect two building models together at the top floor along with the line passing through the center of each building. A harmonic load of constant amplitude was applied at the first floor of Building I, parallel to the damper, to have a swept test from 0·5 to 20 Hz at a very low velocity. The resulting normalized frequency response curve obtained from sensor A3 (at the top of Building I) is displayed in Figure 7. The four natural frequencies of 3·24, 8·40, 12·30 and 12·65 Hz, were identified. The harmonic load was then applied at the first floor of Building II to have another swept test. The measured normalized frequency response curve from sensor A6 (at the top of Building II) is also shown in Figure 7, from which the four natural frequencies of 3·24, 5·36, 12·65 and 19·18 Hz were identified. Among the identified eight frequencies, three natural frequencies of 3·24, 8·40 and 12·30 Hz originated from Building I while the natural frequencies of 5·36, 12·65 and 19·18 Hz came from Building II. The installation of the fluid damper made the two

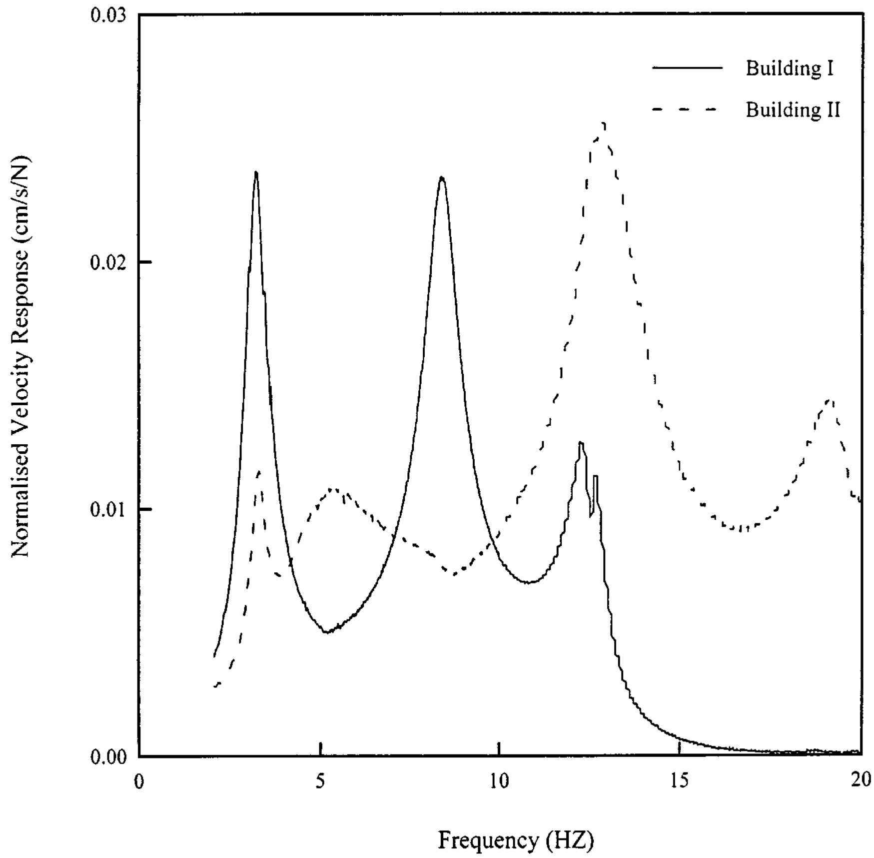

Figure 7. Frequency response curves of adjacent buildings with fluid damper

buildings be partially coupled, as implied by the response peak of Building II at a frequency of 3·24 Hz and the response peak of Building I at a frequency of 12·65 Hz. Compared with the natural frequencies of individual buildings, one may observe that the installation of fluid damper moderately increased the first natural frequency of each building but did not affect higher natural frequencies of the buildings.

The modal damping ratios (including the structural damping ratio) were identified from these response curves as 8·5, 30·0, 5·7 and 4·5 per cent for the first, second, third, and sixth modes, respectively. The modal damping ratios in the fourth and fifth modes were hardly identified since they are closely spaced. Obviously, the installation of the fluid damper enhanced the modal damping ratios significantly, in particular, in the first and second modes of vibration. Thus, it can be expected that the dynamic response of both buildings can be significantly reduced.

From the tests, it was found that the mode shapes of the fluid damper-adjacent building system depended on the position of external excitation. For the harmonic load applied to Building I, the measured mode shape matrixes for Buildings I and II at the natural frequencies of 3·24, 8·40 and

12·30 Hz are as follows:

$$[\Psi]_1 = \begin{bmatrix} 1{\cdot}000 & 1{\cdot}000 & 1{\cdot}0000 \\ 1{\cdot}683 & 0{\cdot}481 & -1{\cdot}225 \\ 2{\cdot}313 & -0{\cdot}777 & 0{\cdot}603 \end{bmatrix}, \quad [\Psi]_2 = \begin{bmatrix} 0{\cdot}440 & 0{\cdot}226 & 0{\cdot}453 \\ 0{\cdot}871 & 0{\cdot}308 & 0{\cdot}272 \\ 1{\cdot}176 & 0{\cdot}184 & -0{\cdot}305 \end{bmatrix} \tag{14}$$

The above mode shapes were normalized based on the first floor of Building I. Compared with the mode shape matrixes of Building I without fluid damper, the mode shape matrixes of Building I with fluid damper changed only slightly. The associated mode shapes of Building II, however, did not always follow those of either Building I or Building II without fluid damper. The modal motion of Building II was also found to have a phase difference from that of Building I. For the harmonic load applied to Building II, the measured mode shape matrixes for Buildings II and I at the natural frequencies of 5·36, 12·65 and 19·18 Hz, which were normalized based on the first floor of Building II, are as follows:

$$[\Psi]_1 = \begin{bmatrix} 0{\cdot}435 & 0{\cdot}254 & 0{\cdot}003 \\ 0{\cdot}562 & -0{\cdot}300 & -0{\cdot}011 \\ 0{\cdot}376 & 0{\cdot}229 & 0{\cdot}063 \end{bmatrix}, \quad [\Psi]_2 = \begin{bmatrix} 1{\cdot}000 & 1{\cdot}000 & 1{\cdot}000 \\ 1{\cdot}367 & 0{\cdot}531 & -1{\cdot}200 \\ 1{\cdot}663 & -0{\cdot}799 & 0{\cdot}571 \end{bmatrix} \tag{15}$$

Compared with the mode shapes of Building II without fluid damper, the first mode of Building II with fluid damper was moderately changed but the higher modes of vibration were only slightly altered. The associated modal shapes of Building I, however, did not follow the mode shapes of Building I without fluid damper. The associated model motion of Building I also had a phase difference from that of Building II. The above discussion indicates that the mode shape of the fluid damper-adjacent building system depends on the position of external excitation. The coupled system studied here is no longer a classically damped system.

Similar tests were carried out on the system for different damper damping coefficients to see the variations of system modal damping ratio and natural frequency with damper damping coefficient. The different damper damping coefficient was achieved by adjusting the gaps between the damper piston and rectangular box and was measured during the tests of the system. Figures 8(a)–8(d) show the variations of the first, second, third and sixth modal damping ratios with damper damping coefficient. It is seen that there was an optimal damper damping coefficient around 3500 N s/m by which the maximum modal damping ratios could be obtained in the first and second vibration modes. The third and sixth modal damping ratios, however, increased almost monotonically with increasing damper damping coefficient. The fourth and fifth modal damping ratios were hardly estimated since these two modes were coupled. It is encouraging to see that because of the installation of fluid damper, the modal damping ratio in the first mode of vibration could be increased to about 8·5 per cent and the modal damping ratio in the second mode of vibration could be increased to about 30 per cent. The reason why the second modal damping ratio can be enhanced much higher than other modes may be related to the stiffness ratio of two buildings and the location of fluid damper.

Figures 9(a)–9(d) display viriations of the first to sixth natural frequencies with damper damping coefficient. Apart from the second natural frequency, all other natural frequencies remained almost constant. The second natural frequency, however, moderately increased with increasing damper damping coefficient.

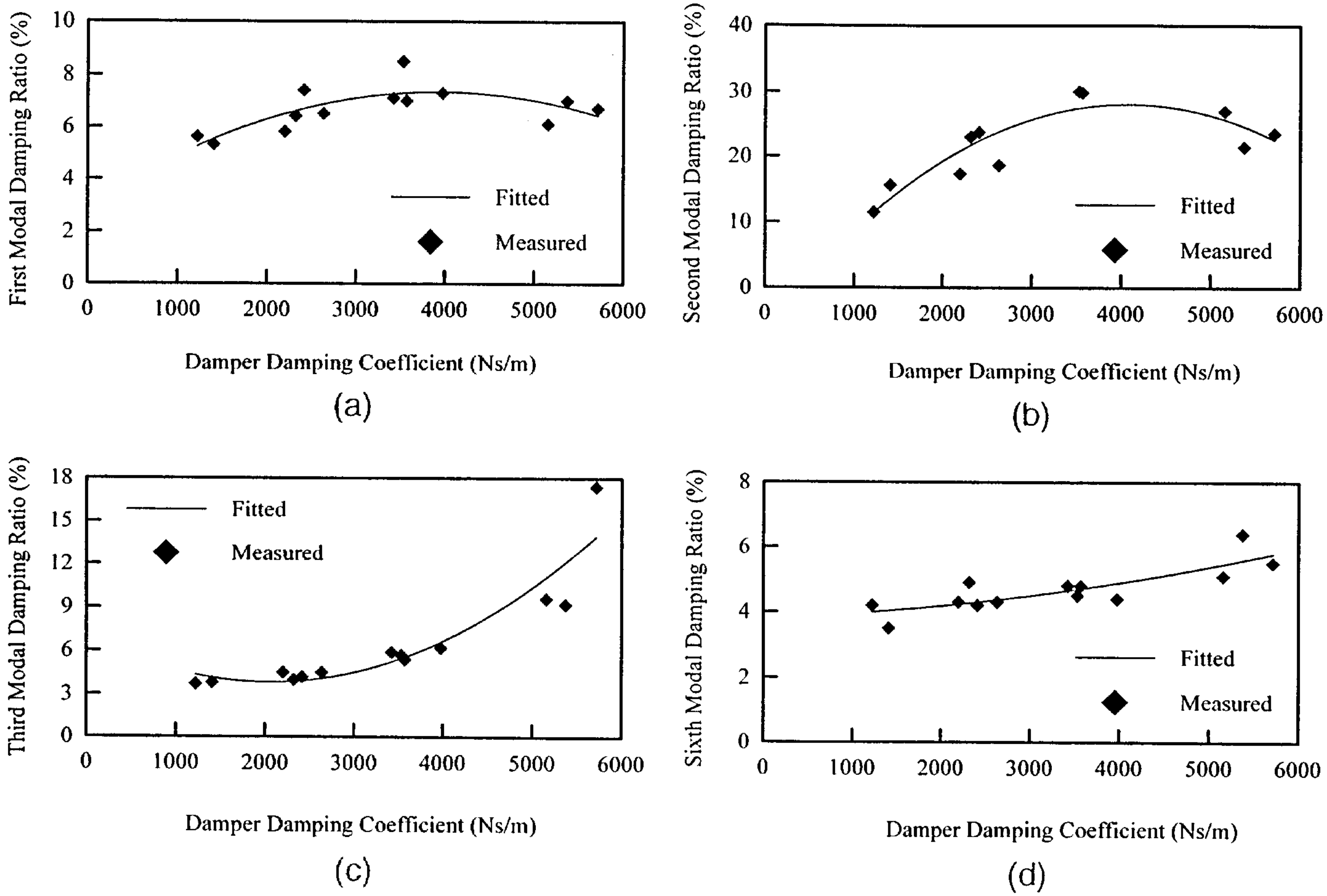

Figure 8. Variations of modal damping ratio of adjacent buildings with damper at top floor: (a) first modal damping ratio; (b) second modal damping ratio; (c) third modal damping ratio; (d) sixth modal damping ratio

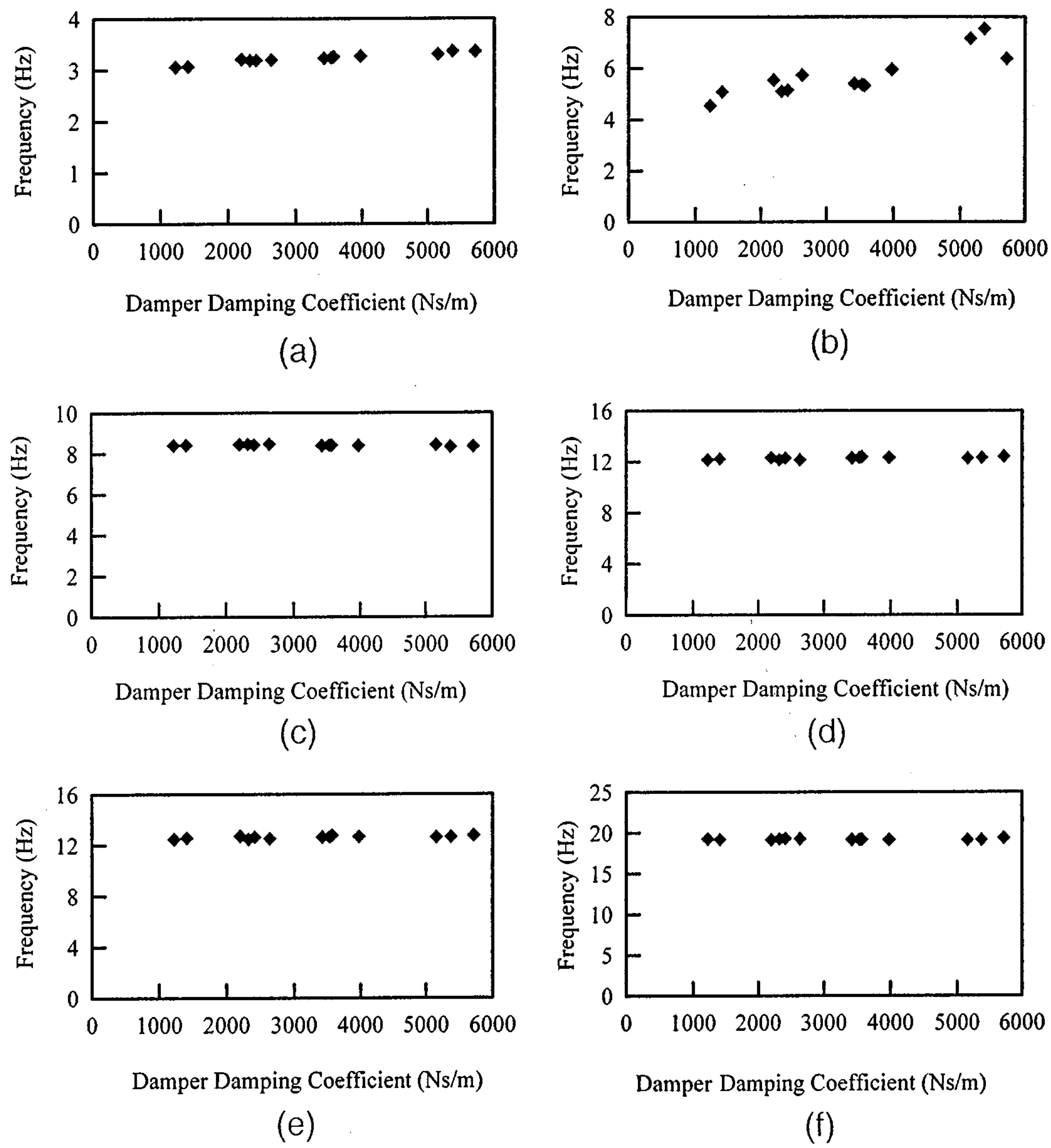

Figure 9. Variations of natural frequency of adjacent buildings with damper at top floor: (a) first natural frequency; (b) second natural frequency; (c) third natural frequency; (d) fourth natural frequency; (e) fifth natural frequency; (f) sixth natural frequency

Fluid damper at second floor

After the tests on the adjacent buildings with a fluid damper installed at the top floor were finished, the fluid damper was then moved to the second floor of the adjacent buildings. Two swept harmonic tests were then carried out for any given damper damping coefficient. In one test,

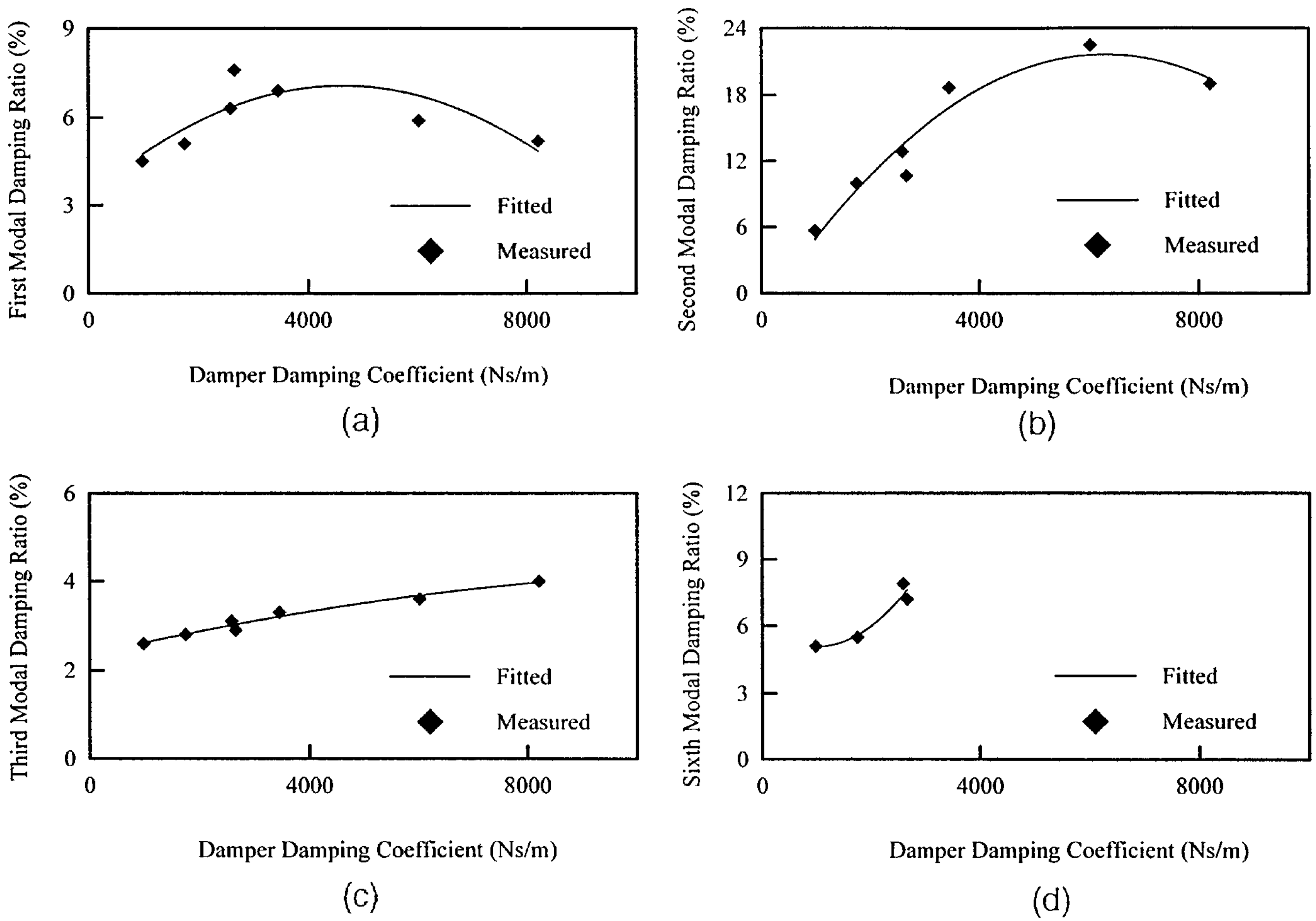

Figure 10. Variations of modal damping ratio of adjacent buildings with damper at second floor: (a) first modal damping ratio; (b) second modal damping ratio; (c) third modal damping ratio; (d) sixth modal damping ratio

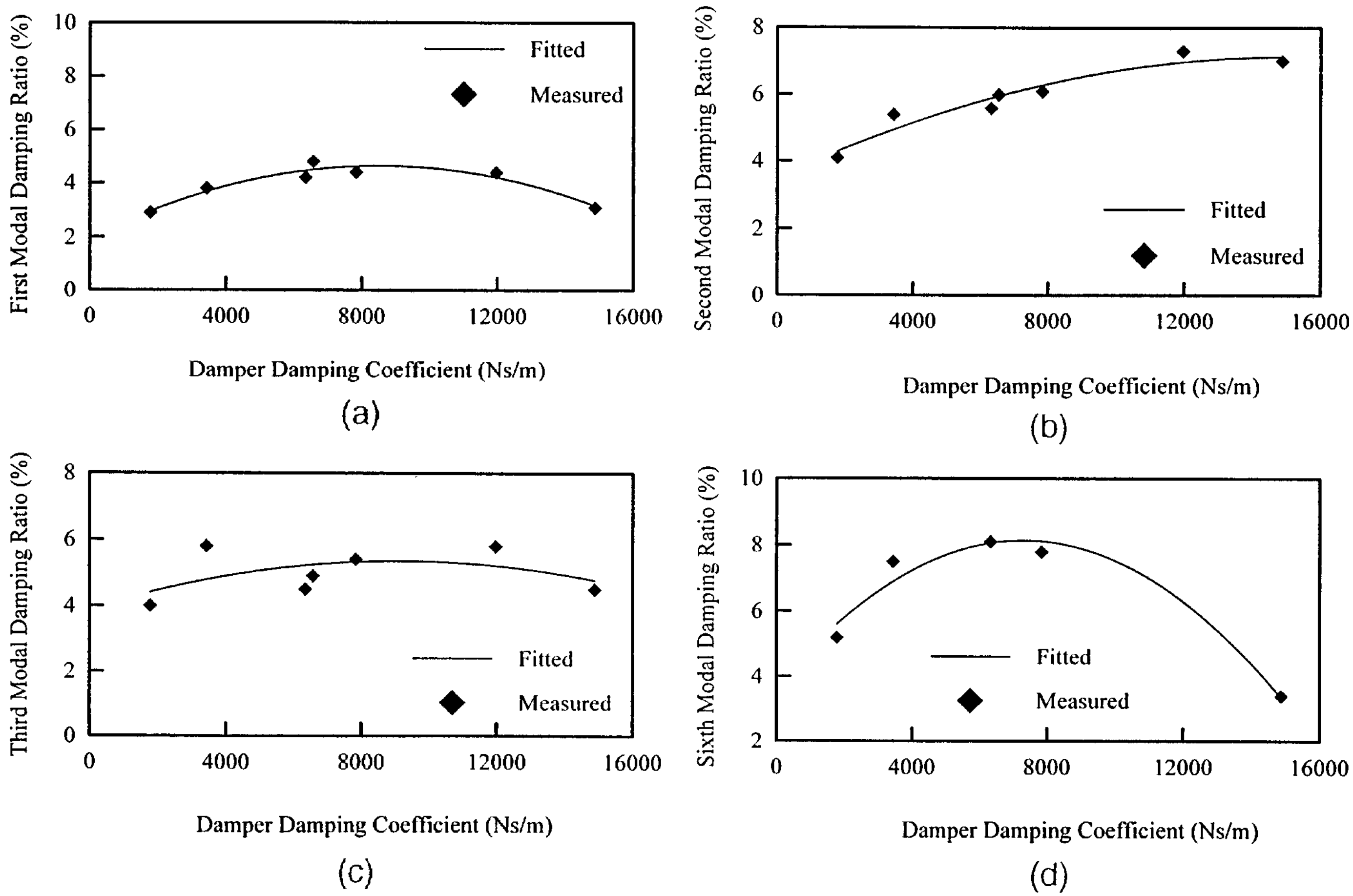

Figure 11. Variations of modal damping ratio of adjacent buildings with damper at first floor: (a) first modal damping ratio; (b) second modal damping ratio; (c) third modal damping ratio; (d) sixth modal damping ratio

the harmonic load of constant amplitude was applied at the first floor of Building I while in the other test, the load was applied at the first floor of Building II. In terms of the measured frequency response curves of the two buildings and the measured displacement and force response curves of the damper, the variations of modal damping ratio and natural frequency of the system with damper damping coefficient were observed.

Figures 10(a)–10(d) show the variation of the first, second, third and sixth modal damping ratio with damper damping coefficient. The optimal damper damping coefficient for the first vibration mode was about 3454 N s/m but for the second mode of vibration of optimal value was about 6025 N s/m. The achievable maximum modal damping ratio was about 7 per cent for the first mode of vibration and 20 per cent for the second mode of vibration. For the sixth mode of vibration, when damper damping coefficient was increased to more than 3400 N s/m, the resonant response around the sixth natural frequency almost disappeared due to high damping and thus the corresponding modal damping ratio could not be estimated. The third modal damping ratio, however, increased slightly with the increasing damper damping coefficient.

Compared with the achievable maximum modal damping ratios obtained when the fluid damper was installed at the top floor, the achievable maximum modal damping ratios of the adjacent buildings with the fluid damper installed at the second floor were smaller in the first three modes of vibration. This is because the damper at the second floor was not located at the maximum amplitude of the first and second modes of the system and also because it was close to the node of the third vibration mode of the system.

Similar to the fluid damper installed at the top floor, all the natural frequencies, apart from the second natural frequency, remained almost constant within a wide range of damping coefficient. The second natural frequency increased with the increasing damper damping coefficient.

Fluid damper at first floor

Figures 11(a)–11(d) show the variations of the first, second, third, and sixth modal damping ratios of the system with the damping coefficient of the damper installed at the first floor of the buildings. The optimal damper damping coefficient for the first vibration mode was increased to about 6500 N s/m, and for the second vibration mode it was increased to about12 000 N s/m. These optimal damper damping coefficients were much higher than those obtained when the fluid damper was installed either at the second floor or the top floor. The corresponding achievable maximum damping ratio was about 4·5 per cent for the first mode and 7 per cent for the second mode, which were smaller than those achieved when the damper was installed at the top floor and the second floor. For the third and sixth modes of vibration, there also existed some optimal damper damping coefficients by which the third and sixth modal damping ratios of the system could reach about 6 and 8 per cent, respectively. Clearly, the position of fluid damper did affect the performance of the damper.

COMPARISON OF DYNAMIC RESPONSE

Fluid damper at top floor

When a fluid damper was installed at the top floor of the adjacent buildings, its optimal damping coefficient was 3531 N s/m for the first vibration mode, and the associated modal

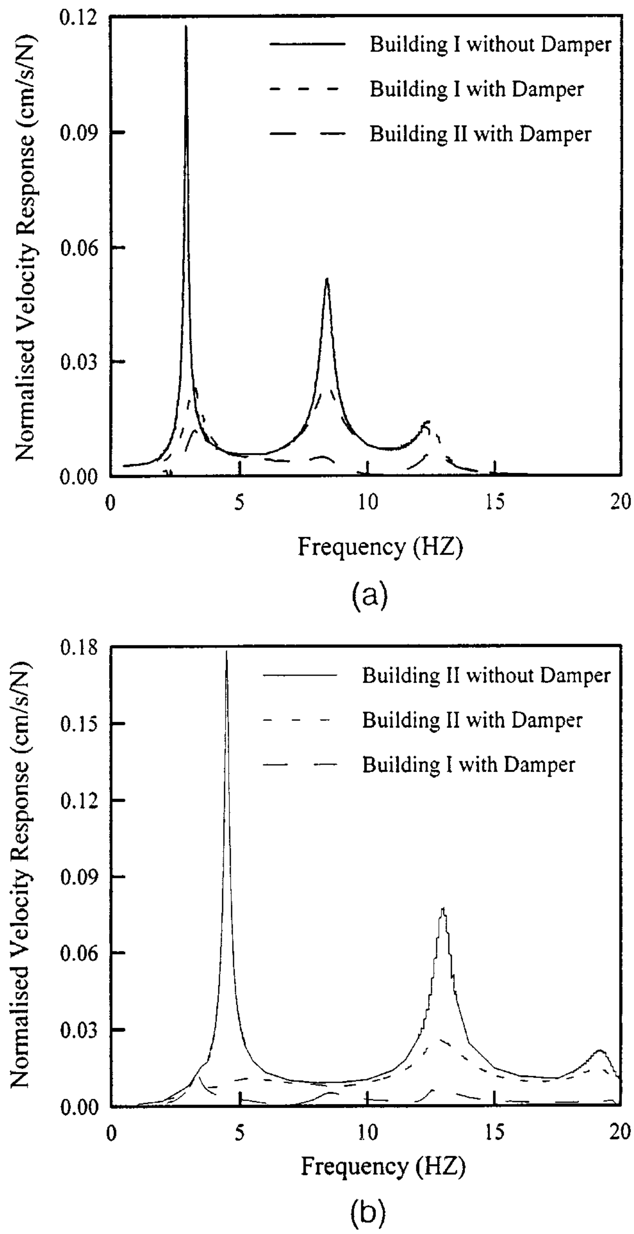

Figure 12. Frequency response curves of adjacent buildings with damper at top floor: (a) building I excited; (b) building II excited

damping ratios in the first and second vibration modes of the system were 8·5 and 30·0 per cent, respectively. For such a case, a harmonic load of constant amplitude was first applied at the first floor of Building I to have a swept test from 0·5 to 20 Hz. The measured normalized frequency response curve at the top floor of Building I was compared with the measured normalized

frequency response curve at the top floor of Building I without fluid damper (see Figure 12(a)). Clearly, because of the fluid damper the peak responses at the first and second natural frequencies of Building I without fluid damper were tremendously reduced. The ratio of the first peak response of Building I with to without the fluid damper was about 1/6 and the ratio of the second peak response was over 1/2. The frequency response curve at the top floor of Building II due to the excitation at Building I is also plotted in Figure 12(a). It is seen that the peak responses of Building II were much smaller than those of Building I with the fluid damper.

The harmonic load of constant amplitude was then applied to the same system at the first floor of Building II to have another swept test from 0·5 to 20 Hz. The measured frequency response curve at the top floor of Building II with the fluid damper is plotted in Figure 12(b) together with the frequency response curve at the top floor of Building II without fluid damper. It is seen that the first peak response of Building II without fluid damper was almost completely suppressed, leading to a ratio of the peak response with to without the fluid damper about 1/18. This is consistent with the results from the modal damping ratio measurement. The second peak response of Building II without the fluid damper was also reduced significantly, resulting in a peak response ratio over 1/2. The frequency response curve at the top floor of Building I due to the excitation at Building II is also plotted in Figure 12(b). Clearly, the peak response of Building I were much smaller than those of Building II with the fluid damper.

From the above discussion, one may conclude that the fluid damper of proper damping coefficient installed at the top floor of the buildings can tremendously reduce the peak responses of either building subject to harmonic loading.

Fluid damper at second floor

For the building-damper system with a fluid damper of 2657 N s/m damping coefficient installed at the second floor, the harmonic excitation was applied to the first floor of Building I to have a swept test. The measured frequency response curve at the top floor of Building I is shown in Figure 13(a) together with the frequency response curve of Building II at the top floor with fluid damper and the frequency response curve of Building I at the top floor without fluid damper. Clearly, because of the fluid damper, the first peak response of Building I without the fluid damper was reduced significantly. The second peak response of Building I without the fluid damper was, however, only moderately reduced. This is because the damping ratio in this mode attributed to the fluid damper was small and the position of the fluid damper was also near the node of the second mode of vibration of Building I. From Figure 13(a), it is also seen that the dynamic response of Building II due to the excitation at Building I was quite small, for the most vibration energy was absorbed by the fluid damper before it passed to Building II.

The harmonic load of constant amplitude was then applied to Building II at its first floor. The measured frequency response curve at the top floor of Building II is shown in Figure 13(b) together with the damping response curves at the top floor of Building I with the fluid damper and the top floor of Building II without fluid damper. It is seen that the first peak response of Building II without the fluid damper was reduced tremendously and the second peak response was reduced only moderately. The third peak response of Building II without the fluid damper was almost completely suppressed. It is also seen that the dynamic response of Building I due to the excitation at Building II was very small but the harmonic excitation at Building II did excite out the first peak response of Building I through the fluid damper.

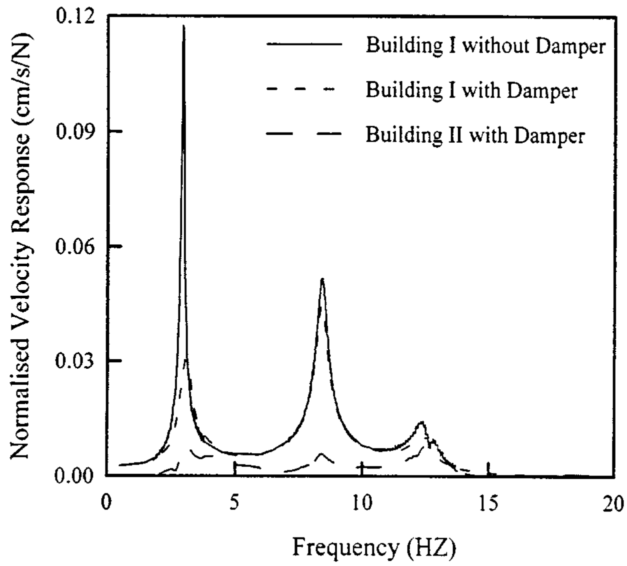

(a)

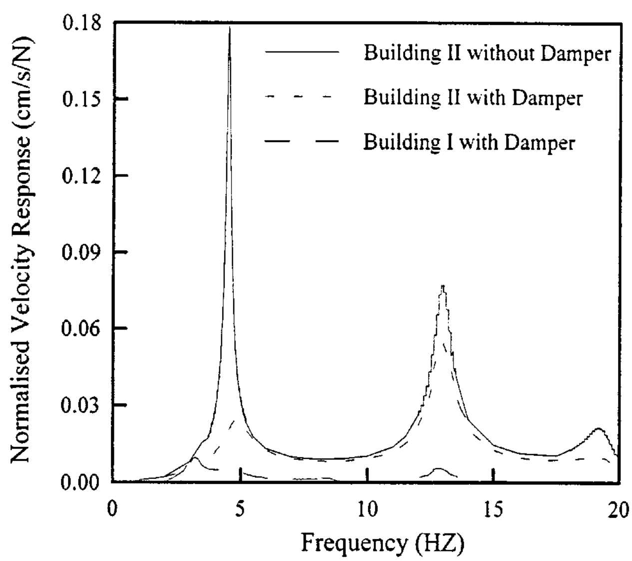

(b)

Figure 13. Frequency response curves of adjacent buildings with damper at second floor: (a) building I excited; (b) building II excited

Fluid damper at first floor

Figure 14(a) shows the frequency response curves at the top floor of Building I with and without the fluid damper and the frequency response curve at the top floor of Building II with the

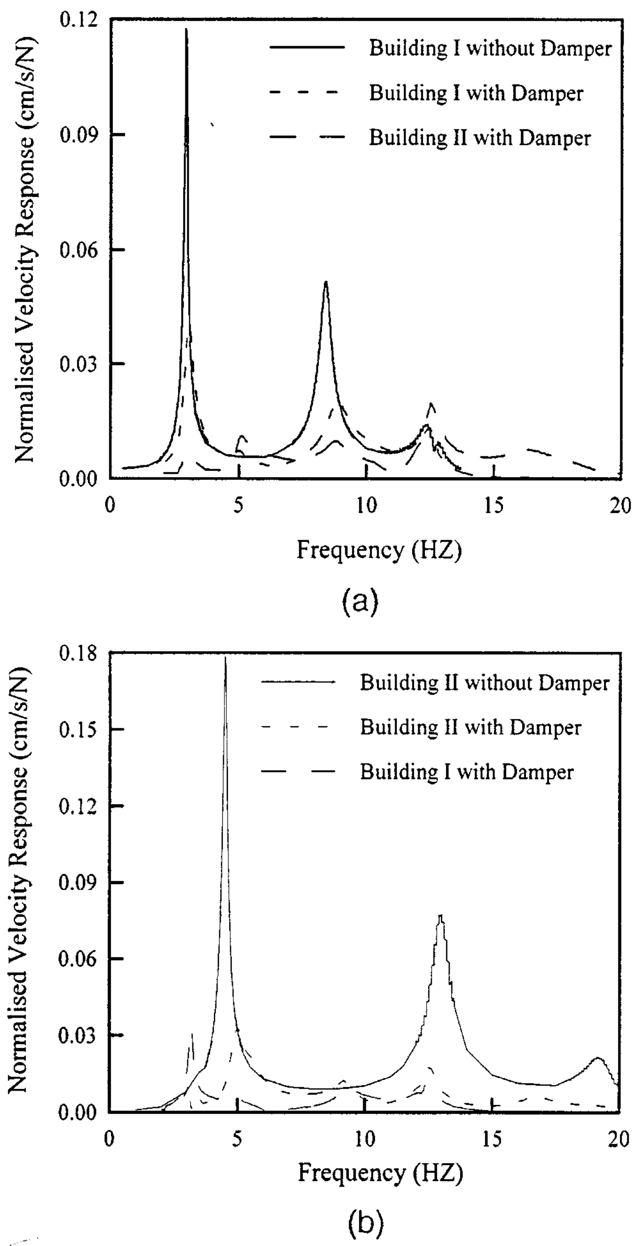

Figure 14. Frequency response curves of adjacent buildings with damper at first floor: (a) building I excited; (b) building II excited

fluid damper from the case where the first floor of Building I was excited. Figure 14(b) shows the frequency response curves at the top floor of Building II with and without the response damper and the frequency response curve at the top floor of Building I with the fluid damper from the

case where the first floor of Building II was excited. The damping coefficient of the fluid damper used was about 6500 N s/m, which was the optimal value for the first mode of vibration of the system. It is seen from the figures that the peak responses of Building I and Building II were significantly reduced because of the installation of the fluid damper.

However, the position of the fluid damper at the first floor was far away from the maximum amplitude of the first vibration mode of each building. Thus, the effectiveness of the fluid damper installed at the first floor on the reduction of the first peak response of each building was relatively smaller, compared with the fluid damper installed at the top floor and the second floor. Nevertheless, the fluid damper installed at the first floor could reduce the second peak response of individual building more than the fluid damper installed at the second floor. In particular, when the fluid damper was installed at the first floor and the external excitation was also applied at the first floor, the building coupling was relatively easily identified. For instance, from the frequency response curve of Building II with the fluid damper in Figure 14(a), the first six natural frequencies of the system could be identified even though the excitation was applied at Building I. From the frequency response curve of Building I with the fluid damper shown in Figure 14(b), the first peak response of Building I was almost the same as that of Building II due to the structural coupling.

Comparing the frequency response curves obtained from the three locations of the fluid damper, one may find that the optimal position of fluid damper to suppress the first and second peak responses of each building subject to harmonic loading was at the top floor.

CONCLUSIONS

An experimental investigation has been carried out on dynamic characteristic and dynamic response of adjacent buildings connected by a fluid damper at different positions. The two model buildings were constructed as three-storey shear buildings, and the fluid damper was designed as a linear viscous damper of its damping coefficient being adjustable. The natural frequencies, mode shapes, modal damping ratios, and dynamic responses to harmonic excitation of the adjacent buildings with and without the fluid damper connected were determined. The optimal damping coefficient and location of the fluid damper for achieving the maximum modal damping ratio and the maximum reduction of dynamic response of both buildings were identified. The interaction of the fluid damper with the inherent properties of the buildings was observed. The experimental results showed that the overall performance of the fluid damper-building system could be significantly enhanced using the fluid damper of proper parameter to connect the adjacent buildings. The performance of the fluid damper-building system to earthquake excitation will be investigated at a late stage when the shaking table facility is available.

ACKNOWLEDGEMENTS

The writers are grateful for the financial support from the Hong Kong Polytechnic University through its Area of Excellence Program as well as a HKPU research grant. The writers also very much appreciate the help from Mr Craig Winters from Taylor Devices, Inc., U.S.A. in providing us with their sample fluid dampers and useful information.

REFERENCES

1. K. Seto and Y. Matsumoto, 'A structural vibration control method of flexible buildings in response to large earthquakes and strong windes', *Proc. 2nd Int. Workshop on Structural Control*, Hong Kong, 1996, pp. 490–496.
2. Y. Yamada, N. Ikawa, H. Yokoyama and E. Tachibana, 'Active control of structures using the joint member with negative stiffness', *Proc. 1st World Conf. on Structural Control,* Los Angeles, California, U.S.A., Vol. 2, TP2, 1994, pp. 41–49.
3. K. Gurley, A. Kareem, L. A. Bergman, E. A. Johnson and E. Klein, 'Coupling tall buildings for control of response to wind', in Schueller, Shinozuka and Yao (eds), *Structural Safety & Reliability*, Balkema, Rotterdam, 1994, pp. 1553–1560.
4. Y. L. Xu, Q. He and J. M. Ko, 'Dynamic response of damper-connected adjacent buildings under earthquake excitation', *Engng. Struct.* **21**, 135–148 (1999).
5. M. C. Constantinou and M. D. Symans, 'Seismic response of structures with supplemental damping', *Struct. Des. Tall Buildings* **2**, 77–92 (1993).
6. M. C. Constantinou and M. D. Symans, 'Experimental and analytical investigation of seismic response of structures with supplemental fluid viscous dampers', *Technical Report NCEER-92-0032*, National Center for Earthquake Engineering Research, State University of New York at Buffalo, Buffalo, U.S.A., 1992.